ISSN 0915-633X

NATIONAL INSTITUTE FOR FUSION SCIENCE

Microstructure and Mechanical Property of Neutron Irradiated TiNi Shape Memory Alloy

Y. Matsukawa, T. Suda, S. Ohnuki and C. Namba

(Received - Nov. 20, 1997)

NIFS-534 Jan. 1998

RESEARCH REPORT
NIFS Series

NAGOYA, JAPAN

Microstructure and Mechanical Property of Neutron Irradiated TiNi Shape Memory Alloy

Y.Matsukawa※, ※※, T.Suda※, S.Ohnuki※ and C.Namba※※

※ *Faculty of Engineering, Hokkaido University, Sapporo N-13 W-8, 060, Japan*
※※*National Institute for Fusion Science, Toki, 509-52, Japan*

Abstract

Microstructure and mechanical property of neutron irradiated TiNi shape memory alloy have been investigated. The doses were on the order of 10^{20} to 10^{23}n/m^2. All of the irradiation was performed below 423K. Amorphization was confirmed after the irradiation of 1.2×10^{23}n/m^2. The recovery behavior of the applied strain was drastically changed after the irradiation. The breaking point of the stress-strain curve, σ_M, increased with increasing dose. These results indicate that amorphous phase dominates the suppression of the martensitic transformation, and causes the change in mechanical property.

keywords : shape memory alloy, neutron irradiation, mechanical property, microstructure, amorphization, martensitic transformation

1. Introduction

TiNi shape memory alloy is expected to be used in nuclear reactor environment[1]. Many researchers have examined the stability of the mechanical property during neutron irradiation. The previous work has revealed that TiNi irradiated with high energy particles showed some peculiar behavior[2-4]. Differential Scanning Calorimetry (DSC) measurements revealed that the martensitic and its inverse transformation temperatures (Ms and Af point) shifted to the lower temperature side[2,3]. An extraordinary pseudoelastic behavior was observed in TiNi irradiated at high dose[2,4]. These results implied that the shape memory effect and the pseudoelasticity were affected by high energy particles irradiation, however, the mechanism is not fully understood at this point. On the other hand, TiNi is well known as the intermetallic compound in which amorphization occurs during electron irradiation[5,6]. The correlation between such irradiation-induced microstructural change and the change in mechanical property has not been discussed enough.

In the present study, both microstructure and the mechanical properties of neutron irradiated TiNi shape memory alloy have been investigated. The primary concern is to clarify the mechanism whereby the mechanical property changes after neutron irradiation.

2. Experiments

Three kinds of TiNi alloy with different composition and transformation temperatures, were used for this experiment. They were kindly supplied by the Japan Stainless Steel Ltd. Co. Electron Probe Micro Analyzer (EPMA) revealed their composition were Ti-50.0, 51.0 and 51.5 at.%Ni. The transformation temperatures and the structure at room temperature before irradiation are shown in Table 1. The all neutron irradiation was performed at Japan Materials Testing Reactor (JMTR). The alloys were delivered as sheets with thickness of 0.2mm. They were cut into discs with diameters of 3mm and tensiles with size of 16mm $\times$4mm. The doses were 1.4×10^{20}, 1.3×10^{22} and 1.2×10^{23}n/m^2. The irradiation temperature was below 423K, and the alloys were kept at this temperature during the irradiation for 0.6ks, 3.6ks and 515.4ks,

respectively.

After the irradiation, the microstructure was observed by 200keV Transmission Electron Microscope (TEM) at room temperature. Tensile tests were performed at room temperature with strain rate of 2.8×10^{-4}/s. Differential Thermal Analysis (DTA) was performed in order to check the transformation temperature after the irradiation. Since the temperature range can be measured by DTA was only above room temperature, we measured only the inverse transformation temperature of Ti-50.0at.%Ni. The heating rate was 10K/s.

3. Results

3.1 Microstructure

Fig.1 shows typical microstructures and corresponding electron diffraction patterns for each dose. In each of the three compositions, there was no obvious microstructural change after the irradiation of up to 1.3×10^{22}n/m^2. However, a halo ring appeared in the diffraction pattern of each alloys after an irradiation of 1.2×10^{23}n/m^2. This means that amorphization was induced by the neutron irradiation.

Fig.2 shows the dark field image from the halo ring. The amorphous phase was confirmed as fine particles with the diameters of 10Å order.

With respect to Ti-51.5at.%Ni irradiated at 1.2×10^{23}n/m^2, many extra diffraction spots besides B2 reciprocal lattice spots were also observed. Fig.3 shows the diffraction pattern of this alloy in the $[100]_{B2}$ zone. Both (a) and (b) were observed in the same specimen. We will mention these extra spots in section 4.4.

Table.1 Composition, Ms point, Af point and structure at room temperature before neutron irradiation of alloys. Composition was revealed by means of EPMA.

Composition	Ms	Af	Structure at R.T.
Ti - 50.0 at.%Ni	337K	373K	B19' Martensite
Ti - 51.0 at.%Ni	298K	338K	B2
Ti - 51.5 at.%Ni	267K	308K	B2

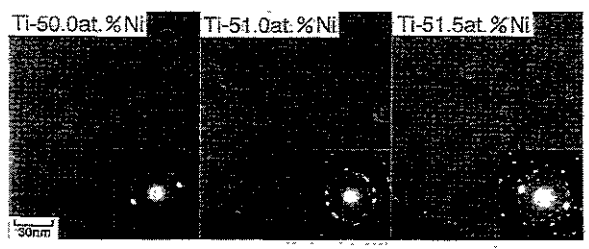

Fig.2 Dark field image from the halo ring of the alloys irradiated at 1.2×10^{23}n/m^2.

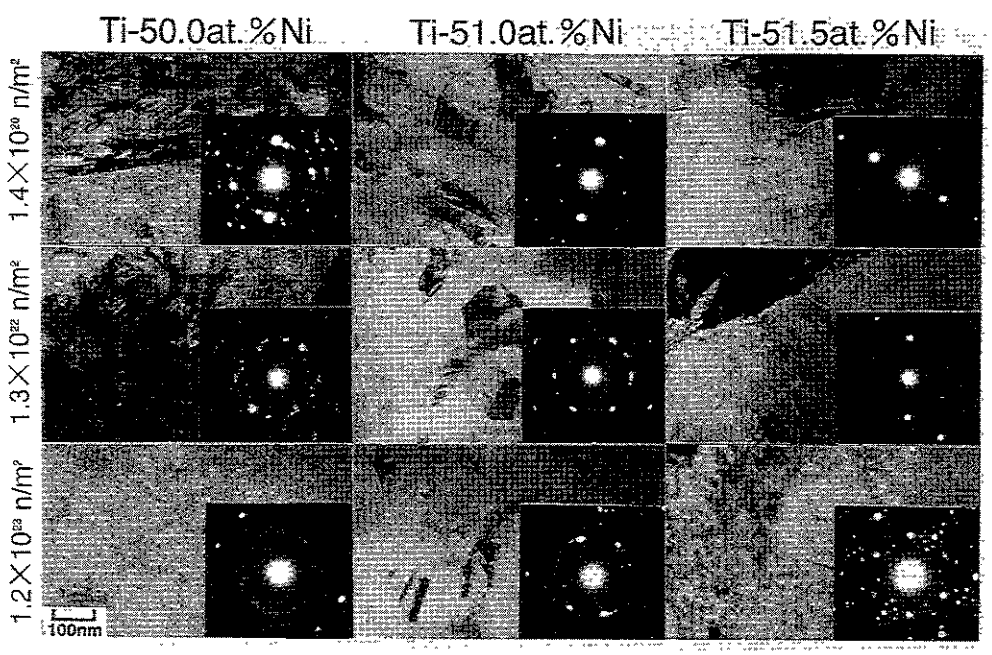

Fig.1 Microstructure and corresponding electron diffraction pattern of neutron irradiated TiNi. Neutron doses were 1.4×10^{20}, 1.3×10^{22} and 1.2×10^{23}n/m^2. All irradiation was performed below 423K.

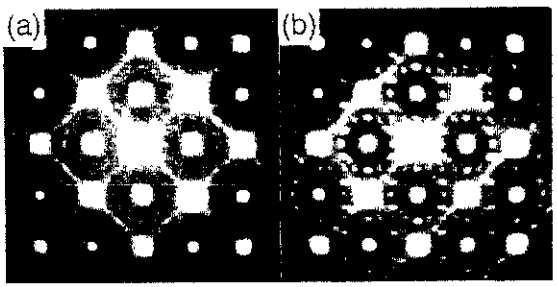

Fig.3 $[100]_{B2}$ zone diffraction pattern of Ti-51 5at.%Ni irradiated at 1.2×10^{23}n/m^2. The irradiation temperature was below 423K Both (a) and (b) were observed in the same specimen

3 2 Mechanical Property

Fig 4 illustrates the stress-strain curve in which the alloys were strained up to 5% and then the applied stress released In Ti-50.0 and 51.0at %Ni samples irradiated up to 1.3×10^{22}n/m^2, a strain of approximately 2% remained after releasing the applied stress. The strain of 2% also remained in unirradiated Ti-51 5at %Ni, however, the strain almost completely recovered in irradiated alloys This implies that Ti-51 5at.%Ni showed pseudoelasticity after the irradiation.

After the irradiation of 1.2×10^{23}n/m^2, the strain was recovered almost completely by releasing the applied stress irrespective of alloy's composition This behavior is just the pseudoelasticity from the viewpoint of strain recovery, however, the strain hysterisis was quite less than the one in conventional pseudoelasticity

Fig 5 illustrates the plot of σ_M, which is the breaking point of the stress-strain curve, at each of the doses. It is obvious that σ_M increased as the dose increased In case of a shape memory alloy, σ_M is not the yield stress. It is the critical stress associated with the martensitic transformation in this alloy [7] Therefore, the increase in σ_M would indicates the suppression of the martensitic transformation

3.3 Transformation Temperature

Fig.6 shows the DTA curve of unirradiated and neutron irradiated Ti-50.0at.%Ni. Since these are the curves during the heating process, the peaks of the curve depend on the inverse martensitic transformation

The peaks slightly shifted from the initial site to the lower temperature side and split after irradiation at low dose There is no peak at the highest dose Comparing the peaks of the irradiation of 10^{20} and 10^{22} n/m^2, their deviation from the initial site were almost the same, and total amount of heat decreased with increasing dose. Therefore, the peak would vanish at the site without more shifting to the lower side

The largeness of the DTA peak represents the thermal change accompanied by the transformation, namely, it corresponds to the amount of the transformation. Therefore, this result indicates that neutron irradiation suppresses the martensitic transformation

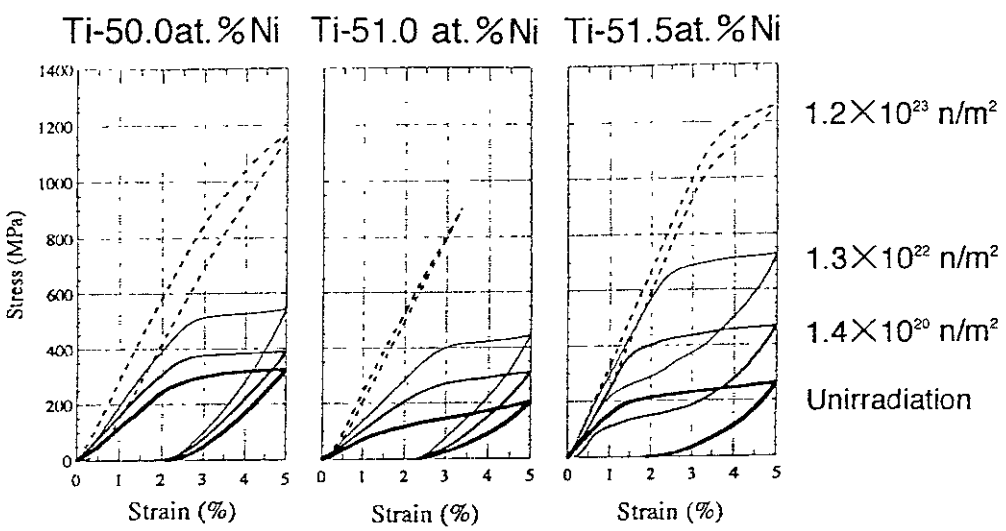

Fig.4 Stress-strain curve of unirradiated and neutron irradiated TiNi Neutron doses were 1.4×10^{20}, 1.3×10^{22} and 1.2×10^{23}n/m^2. All irradiation was performed below 423K

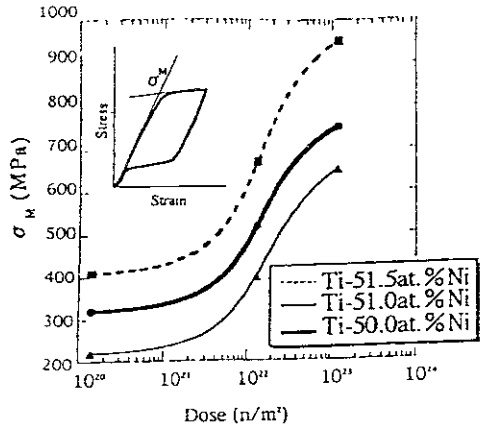

Fig.5 Breaking point of the stress-strain curve, σ_M, of neutron irradiated TiNi at each doses. Neutron doses were 1.4×10^{20}, 1.3×10^{22} and 1.2×10^{23}n/m^2. All irradiation was performed below 423K.

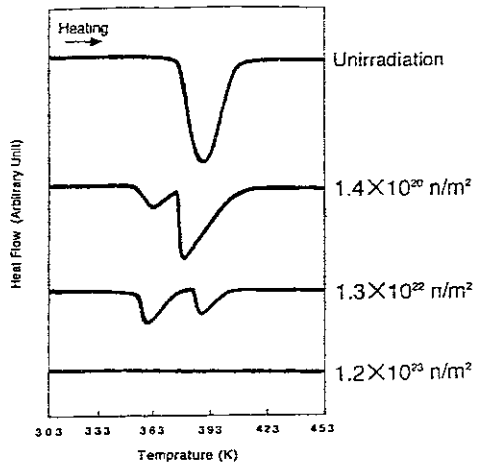

Fig.6 DTA curve during heating of neutron irradiated Ti-50.0at.%Ni. Neutron doses were 1.4×10^{20}, 1.3×10^{22} and 1.2×10^{23}n/m^2. All irradiation was performed below 423K.

4. Discussion

4 1 Suppression of Martensitic Transformation by Amorphous Phase

Microstructural observation revealed that the amorphous phase formed after irradiation, and both results of tensile test and DTA measurement indicated that the martensitic transformation was suppressed in irradiated alloys. It could reasonably be hypothesized that the amorphous phase plays the role of suppressing the martensitic transformation.

Though the amorphous phase was confirmed only after the highest dose in our experiment, however, it would be formed also in an alloy irradiated less than 10^{23}n/m^2. The irradiation temperature and dose rate, which were the predominant factors of irradiation-induced amorphization, were unified in this experiment. Therefore, the extent of the amorphous phase would depend on the dose. The amount of the amorphous phase formed by the irradiation at a lower dose was so small that we could not detect a halo ring in the diffraction pattern. That is the reason why σ_M increased even after the irradiation of less than 10^{23}n/m^2, in which amorphous phase was not confirmed.

The result suggested by A.Kimura et.al[2] supports our hypothesis. The conditions of their irradiation were almost the same as ours. Their DSC analysis showed that the martensitic transformation was suppressed completely after irradiation of 10^{24}n/cm^2 and it recovered after post-annealing at 548K. The temperature of 548K would correspond to the crystallization temperature of the amorphous phase in this alloy.

4.2 Correlation between Amorphization and Chemical Disordering

In general, it is interpreted that the disappearance of Ms and Af peak in DSC (or DTA) curve of neutron irradiated TiNi is caused by a decrease in the degree of the chemical order. The logical basis is as follows; Ms and Af points depend on the alloy' s composition, that is, they decrease with the increase of the compositional deviation from stoichiometry. The deviation brings structural defects, namely, the degree of Bragg-Williams order decrease with an increase of the compositional deviation. Therefore, it is reasonable to understand that the decrease in the degree of order brings a decrease in the Ms and Af points. It was confirmed in the DSC analysis of electron irradiated TiNi that Ms and Af points slightly shifted to lower side after the irradiation[3]. In case of TiNi irradiated neutron at high dose, there was no peak in DSC curve. Based on the logic as mentioned above, the absence of Ms and Af peaks in the DSC curve of neutron irradiated TiNi was interpreted such that they shifted to such an extremely low temperature that they could not be detected. The absence has been believed to result from the complete destruction of the chemical order.

Our DTA measurement suggested the possibility of another mechanism. In our result, DTA peaks vanished at the initial site rather than shifted to the lower

side It is more reasonable to understand that the suppression of the martensitic transformation did not result from the complete destruction of the degree of Bragg-Williams order but from the formation of the amorphous phase Though a slight shift of the peak to the lower side was also confirmed in our experiment, this would be the phenomenon accompanied by amorphization The formation of the amorphous phase, in other words, a topological disorder results in the decrease in the degree of Bragg-Williams order, naturally. Therefore, it is no wonder that a shifting of the DTA peak occurred by amorphization

From the discussion mentioned above, the following conclusion can be made The decrease in the degree of Bragg-Williams order relies on amorphization in this alloy during high energy particle irradiation, at least, under the condition that amorphization is confirmed after the irradiation Therefore, the Ms and Af peaks recovered after post-annealing at the crystallization temperature of the amorphous phase

4 3 Pseudoelastic Behavior of TiNi Irradiated High Dose

Irrespective of the alloy's composition, TiNi irradiated at the highest dose showed extraordinary pseudoelastic behavior, which was almost the same as conventional pseudoelasticity from the viewpoint of recoverable strain but was different in shape from the stress-strain curve. The stress-strain curve of TiNi irradiated at the highest dose was almost linear without strain hysterisis. This extraordinary pseudoelastic behavior is conjectured to be not the pseudoelasticity relying on martensitic transformation but the expansion of recoverable elastic deformation of the B2 phase. The stress-strain curve of Ti-51.5at.%Ni irradiated at the highest dose has a small strain hysterisis, and its elastic deformation enlarged clearly compared with the curves of Ti-51.5at.%Ni irradiated lower dose. Considering the fact that there is no peak in the DTA curve of TiNi irradiated 10^{23}n/m^2, a stress-inducing martensitic transformation would not occur in the TiNi irradiated high dose, either Since it is tremendous that such an extent of strain can recover as elastic deformation, possibly the amorphous phase dispersed in the B2 matrix plays a role in the expansion of the elastic deformation.

In amorphous materials, it is well known that the extent of such a strain can recover elastically Recently, thin foil amorphous TiNi was reported to show the same behavior, too[8]. These facts would support our hypothesis that the change in mechanical properties after neutron irradiation is caused by the formation of the amorphous phase.

A similar pseudoelastic behavior has been observed in cold worked TiNi[9-11], however, the mechanism is different from the one observed in irradiated TiNi In the case of cold worked TiNi, it was revealed that the initial structure before straining was the martensitic phase[10,11], and the behavior relied on reorientation of martensite domain stabilized up to high temperature. Therefore, the recovery mechanism of the applied strain would be different in nature.

4.4 Anomalous Diffraction Spot of Ti-51 5at.%Ni Irradiated at High Dose

As shown in Fig 3, many extra diffraction spots besides B2 were observed in Ti-51.5at.%Ni irradiated at 1.2×10^{23}n/m^2. These diffraction spots are different from the spots of the R phase or metastable phase Ti_3Ni_4[7]. This cannot be explained by the phase transformation known to occur in Ni-rich TiNi with thermal treatment. Therefore, this would be the phase transformation induced by neutron irradiation. We have examined this phase transformation. The detailed analysis will be publish in another paper

5. Conclusion

Microstructural change and the mechanical property of neutron irradiated TiNi were investigated. The results are summarized as follows:

(1) Fine amorphous particles were observed after an irradiation of 1.2×10^{23}n/m^2.

(2) σ_M increased as the dose increased.

These results indicate that the amorphous phase induced by neutron irradiation suppresses the martensitic transformation.

(3) Irrespective of the alloy's composition, the alloy irradiated 1.2×10^{23}n/m^2 showed extraordinary pseudoelastic behavior.

This behavior is not the pseudoelasticity relying on the martensitic transformation but the expanded elastic deformation of the B2 phase. This expansion is supposed to arise from the formation of the amorphous phase by neutron irradiation.

Acknowledgments

The authors thank Dr M.Narui of OB, RIM, Tohoku University for the help with experimental management and assistance

References

(1) M.Nishikawa, T.Narikawa, M.Iwamoto and K.Watanabe : Fusion Technology, 9 (1986) 101-115
(2) A.Kimura, H.Tsuruga, T.Morimura, S.Miyazaki and T.Misawa : Mater. Trans, JIM, 34 (1993) 1076-1082
(3) Y.Nakata, T.Tadaki and K.Shimizu : MRS Int'l. on Adv. Mats. vol.9 (1989) Material Research Society pp.231-236
(4) T.Hoshiya, F.Takada, M.Omi, I.Goto and H.Ando : J. Japan Inst. Metals, 56, No.5 (1992) 502-508 (Japanese)
(5) H.Mori and H.Fujita : J. Appl. Phys. 21 (1982) 494
(6) Y.Matsukawa and S.Ohnuki : J. Nucl. Mat. 239 (1996) 261-266
(7) S.Miyazaki and K.Otsuka : Metall. Trans. 17A, (1986) 53-63
(8) Gyoubu : to be published
(9) G.R.Zando and T.W.Duerig : MRS Int'l. on Adv. Mats. 9 (1989) Material Research Society. 201-206pp.659-664
(10) H.C.Lin and S.K.Wu : Acta metall. mater. 42, No.5, (1994) 1623-1630
(11) H.C.Lin, S.K.Wu, T.S.Chou and H.P.Kao : Acta metall. mater. 39, No.9, (1991) 2069-2080

Recent Issues of NIFS Series

NIFS-497 T Takahashi, Y Tomita, H Momota and Nikita V Shabrov,
Collisionless Pitch Angle Scattering of Plasma Ions at the Edge Region of an FRC, July 1997

NIFS-498 M Tanaka, A Yu Grosberg, V S Pande and T Tanaka
Molecular Dynamics and Structure Organization in Strongly-Coupled Chain of Charged Particles, July 1997

NIFS-499 S Goto and S Kida
Direct-interaction Approximation and Reynolds-number Reversed Expansion for a Dynamical System, July 1997

NIFS-500 K. Tsuzuki, N Inoue, A Sagara, N Noda, O Motojima, T Mochizuki, T Hino and T Yamashina
Dynamic Behavior of Hydrogen Atoms with a Boronized Wall, July 1997

NIFS-501 I Vinar and S Sudo,
Multibarrel Repetitive Injector with a Porous Pellet Formation Unit, July 1997

NIFS-502 V Vdovin, T Watari and A Fukuyama
An Option of ICRF Ion Heating Scenario in Large Helical Device, July 1997

NIFS-503 E Segre and S Kida
Late States of Incompressible 2D Decaying Vorticity Fields, Aug 1997

NIFS-504 S Fujiwara and T Sato,
Molecular Dynamics Simulation of Structural Formation of Short Polymer Chains, Aug 1997

NIFS-505 S Bazdenkov and T Sato
Low-Dimensional Model of Resistive Interchange Convection in Magnetized Plasmas, Sep. 1997

NIFS-506 H Kitauchi and S Kida,
Intensification of Magnetic Field by Concentrate-and-Stretch of Magnetic Flux Lines, Sep 1997

NIFS-507 R L Dewar,
Reduced form of MHD Lagrangian for Ballooning Modes, Sep 1997

NIFS-508 Y.-N Nejoh,
Dynamics of the Dust Charging on Electrostatic Waves in a Dusty Plasma with Trapped Electrons, Sep 1997

NIFS-509 E Matsunaga, T Yabe and M. Tajima,
Baroclinic Vortex Generation by a Comet Shoemaker-Levy 9 Impact; Sep 1997

NIFS-510 C C. Hegna and N Nakajima,
On the Stability of Mercier and Ballooning Modes in Stellarator Configurations; Oct 1997

NIFS-511 K Ohto and T Hatori,
Rotation and Oscillation of Nonlinear Dipole Vortex in the Drift-Unstable Plasma; Oct 1997

NIFS-512 J. Uramoto,
Clear Detection of Negative Pionlike Particles from H_2 Gas Discharge in Magnetic Field, Oct 1997

NIFS-513 T Shimozuma, M Sato, Y. Takita, S. Ito, S Kubo, H Idei, K Ohkubo, T Watari, T S. Chu, K Felch, P Cahalan and C M Loring, Jr,
The First Preliminary Experiments on an 84 GHz Gyrotron with a Single-Stage Depressed Collector, Oct 1997

NIFS-514 T Shimozuma, S Morimoto, M Sato, Y Takita, S Ito, S. Kubo, H Idei, K. Ohkubo and T Watari,
A Forced Gas-Cooled Single-Disk Window Using Silicon Nitride Composite for High Power CW Millimeter Waves, Oct 1997

NIFS-515 K Akaishi,
On the Solution of the Outgassing Equation for the Pump-down of an Unbaked Vacuum System, Oct 1997

NIFS-516 *Papers Presented at the 6th H-mode Workshop (Seeon, Germany)*: Oct 1997

NIFS-517 John L Johnson,
The Quest for Fusion Energy, Oct. 1997

NIFS-518 J Chen, N. Nakajima and M. Okamoto,
Shift-and-Inverse Lanczos Algorithm for Ideal MHD Stability Analysis: Nov 1997

NIFS-519 M Yokoyama, N Nakajima and M Okamoto,
Nonlinear Incompressible Poloidal Viscosity in L=2 Heliotron and Quasi-Symmetric Stellarators Nov 1997

NIFS-520 S. Kida and H. Miura,
Identificaiton and Analysis of Vortical Structures; Nov. 1997

NIFS-521 K. Ida, S. Nishimura T Minami, K Tanaka, S Okamura, M Osakabe, H. Idei, S Kubo C Takahashi and K Matsuoka,
High Ion Temperature Mode in CHS Heliotron/torsatron Plasmas; Nov 1997

NIFS-522 M. Yokoyama, N. Nakajima and M. Okamoto,
Realization and Classification of Symmetric Stellarator Configurations through Plasma Boundary Modulations; Dec 1997

NIFS-523 H. Kitauchi,
Topological Structure of Magnetic Flux Lines Generated by Thermal Convection in a Rotating Spherical Shell; Dec 1997

NIFS-524 T Ohkawa,
Tunneling Electron Trap, Dec 1997

NIFS-525 K. Itoh, S.-I. Itoh, M Yagi, A. Fukuyama,
Solitary Radial Electric Field Structure in Tokamak Plasmas; Dec 1997

NIFS-526 Andrey N. Lyakhov,
Alfven Instabilities in FRC Plasma; Dec 1997

NIFS-527 J. Uramoto,
Net Current Increment of negative Muonlike Particle Produced by the Electron and Positive Ion Bunch-method; Dec 1997

NIFS-528 Andrey N. Lyakhov,
Comments on Electrostastic Drift Instabilities in Field Reversed Configuraiton, Dec 1997

NIFS-529 J. Uramoto,
Pair Creation of Negative and Positive Pionlike (Muonlike) Particle by Interaction between an Electron Bunch and a Positive Ion Bunch; Dec 1997

NIFS-530 J. Uramoto,
Measuring Method of Decay Time of Negative Muonlike Particle by Beam Collector Applied RF Bias Voltage Dec 1997

NIFS-531 J. Uramoto,
Confirmation Method for Metal Plate Penetration of Low Energy Negative Pionlike or Muonlike Particle Beam under Positive Ions, Dec. 1997

NIFS-532 J. Uramoto,
Pair Creations of Negative and Positive Pionlike (Muonlike) Particle or K Mesonlike (Muonlike) Particle in H2 or D2 Gas Discharge in Magnetic Field; Dec. 1997

NIFS-533 S. Kawata, C. Boonmee T. Teramoto L Drska, J Limpouch R. Liska, M. Sinor,
Computer-Assisted Particle-in-Cell Code Development: Dec 1997

NIFS-534 Y. Matsukawa T Suda, S Ohnuki and C Namba,
Microstructure and Mechanical Property of Neutron Irradiated TiNi Shape Memory Alloy, Jan. 1998